

Extended Quantum Spin Liquid with Spinon-like Excitations in an Anisotropic Kitaev-Gamma Model

Matthias Gohlke,¹ Jose Carlos Pelayo,² and Takafumi Suzuki³

¹*Theory of Quantum Matter Unit, Okinawa Institute of Science and Technology Graduate University, Onna-son, Okinawa 904-0495, Japan*

²*Quantum Systems Unit, Okinawa Institute of Science and*

Technology Graduate University, Onna-son, Okinawa 904-0495, Japan

³*Graduate School of Engineering, University of Hyogo, Himeji 671-2280, Japan*

(Dated: December 22, 2022)

The characterization of quantum spin liquid phases in Kitaev materials has been a subject of intensive studies over the recent years, both theoretically and experimentally. Most theoretical studies have focused on an isotropically interacting model with its coupling strength being equivalent on each bond in an attempt to simplify the problem. Here, we study an extended spin-1/2 Kitaev- Γ model on a honeycomb lattice with an additional tuning parameter that controls the coupling strength on one of the bonds: we connect the limit of isolated Kitaev- Γ chains, which is known to exhibit an emergent $SU(2)_1$ Tomonaga-Luttinger liquid phase [Yang et al. Phys. Rev. Lett. **124**, 147205 (2020)], to the two-dimensional model. We report on an instance, in which the Tomonaga-Luttinger liquid persists for finite inter-chain coupling. A quantum spin liquid phase develops in analogy to *sliding Luttinger liquids* that differs from the Kitaev spin liquid. This quantum spin liquid phase features spinon-like excitations similar to those of the antiferromagnetic Heisenberg chain. We use numerical Exact Diagonalization and Density Matrix Renormalization Group on various cluster geometries in a complementary way to overcome finite-size limitations.

Quantum spin liquids (QSL) have become an important research subject in condensed matter physics due to their exotic emergent properties [1–3]. Following the ‘More is different’ philosophy by Anderson [4], competing interactions—or frustration—can give rise to novel emergent features: fractional excitations, topological order, emergent gauge fields, anyonic exchange statistics, etc. Kitaev’s honeycomb model [5] is a paradigmatic spin-1/2 model in this context, due to being exactly solvable and featuring a QSL ground state in terms of itinerant Majorana fermions in a static \mathbb{Z}_2 gauge field. The bond-dependent Kitaev spin-exchange is realized in certain magnets with strong spin-orbit coupling [6]. This mechanism, however, introduces additional spin exchanges [6, 7] that spoil the exact solvability of the Kitaev model. Many candidate Kitaev materials have been proposed [8–11] among which α - RuCl_3 [12] has gained much attention due to a putative QSL phase in an in-plane magnetic field [13, 14], and even more so, since the measurement of a half-quantized thermal hall effect was reported suggesting the existence of emergent Majorana fermions [15–18].

The spin-1/2 Kitaev- Γ (K Γ) model on the honeycomb lattice with ferromagnetic Kitaev exchange and positive symmetric off-diagonal Γ exchange has been proposed as a minimal model for α - RuCl_3 [19–22]. Many different methods have been applied, yet no clear understanding of its quantum ground state has emerged. Among the suggested ground state phases are not only magnetically ordered states, such as zigzag [23], ferromagnet [23–25], six-sublattice [24], or incommensurate spiral order [7, 23, 25], but also quantum paramagnetic phases such as a putative

gapped QSL [26], a lattice-nematic paramagnet [24, 27], or a gapless QSL with multiple Majorana-Dirac nodes [23].

We like to change the perspective and focus instead on an aspect rarely included in theoretical works on Kitaev materials: we additionally tune the strength of the spin exchange spatially, ranging from a limit of uncoupled chains to spatially equal, yet still strongly anisotropic, spin exchange. In fact, such spatial anisotropy may either be intrinsic due to a reduced symmetry of the underlying lattice, such as $C2/m$ [28–31] instead of a full C_3 rotational symmetry, or spatial anisotropy can be induced by applying external pressure or strain [32], which possibly realizes various different QSL [33].

The one-dimensional limit features an emergent Tomonaga-Luttinger liquid (TLL) with the same critical properties as the antiferromagnetic Heisenberg (AFH) chain [34]. Since the TLL is a critical state, most TLLs are unstable under adding small inter-chain coupling [35, 36]. An exception is *sliding Luttinger liquids* [37–39] that occur if the inter-chain coupling competes with the dominant correlations along the chains. As a consequence, long-range order is suppressed.

Here, we argue that a similar mechanism arises in the strongly anisotropic K Γ model: The TLL phase of the K Γ chain turns into an extended QSL phase. This QSL retains the dominant algebraic correlations along the chains and features spinon-like excitations that are characteristic for the AFH chain. This contrasts the emergent Majorana fermions and \mathbb{Z}_2 fluxes of the KSL.

Remarkably, we find the QSL phase with TLL character to extend within a wide range of $\Gamma > 0$ with ferromag-

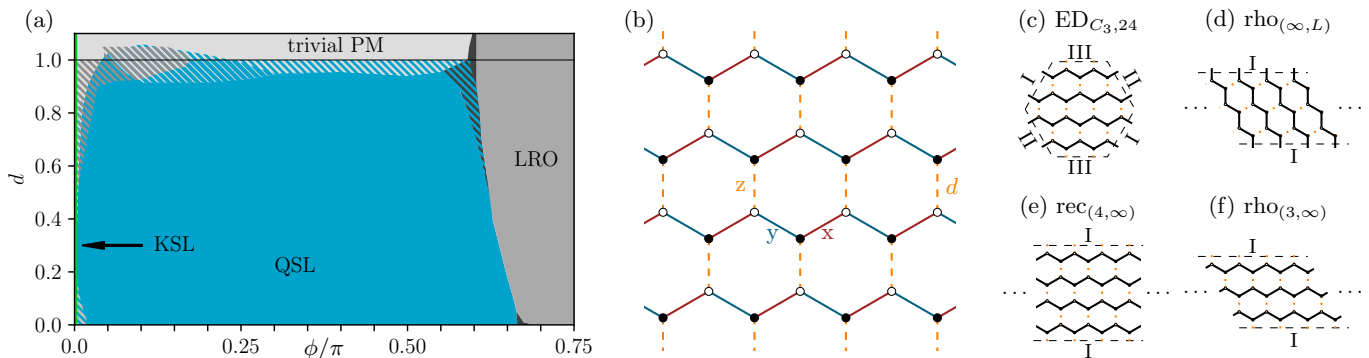


FIG. 1. (a) Schematic ground state phase diagram of the anisotropic K Γ model. The QSL phase is highlighted in blue, while the KSL exist only in a tiny range next to $\phi = 0$. LRO refers to a magnetically ordered phase with non-coplanar 90° order. Hatched areas illustrate where results of DMRG and ED differ. (b) Illustration of the K Γ model on the honeycomb lattice [see Eq. 1] with bond-dependent interactions and additional modification of the coupling along z by a factor d . We use various geometries: (c) C_3 -symmetric 24-site cluster within ED, (d) rhombic unit cell with finite K Γ -chains ($L = \{6, 12, 18\}$) coupled along the infinite direction, (e) rectangular unit cell with four infinite K Γ chains, and (f) rhombic unit cell with three infinite K Γ -chains. Geometries (d-f) are employed within DMRG.

netic Kitaev exchange, and up to the C_3 -symmetric K Γ -model with spatially equal spin-exchange strength (C_3 limit), cf. Fig. 1(a). We base our reasoning on the following key observations upon tuning the inter-chain coupling up to the C_3 limit: (i) absence of a phase transition in a wide range of K/Γ , (ii) absence of a spectral gap, (iii) strong similarities of the dynamical spin-structure factor (DSF) with the AFH chain, and (iv) suppression of the effective inter-chain coupling.

Anisotropic K Γ Model. We consider the spin-1/2 K Γ model on the honeycomb lattice with x , y , and z bonds [see Fig. 1(b)]. Its spin exchange is described by the Hamiltonian

$$\mathcal{H} = -K \sum_{\langle i,j \rangle_{\gamma=x,y}} S_i^\gamma S_j^\gamma + \Gamma \sum_{\langle i,j \rangle_{\gamma=x,y}} \left[S_i^\alpha S_j^\beta + S_i^\beta S_j^\alpha \right] - dK \sum_{\langle i,j \rangle_{\gamma=z}} S_i^\gamma S_j^\gamma + d\Gamma \sum_{\langle i,j \rangle_{\gamma=z}} \left[S_i^\alpha S_j^\beta + S_i^\beta S_j^\alpha \right], \quad (1)$$

where d determines the strength of the K Γ -exchange on the z bond; $d = 1$ refers to equal exchange strength along each bond restoring the C_3 lattice-rotation symmetry, while $d = 0$ refers to the chain limit. Here, we are interested in the range $0 \leq d \lesssim 1$ connecting both limits. Furthermore, we introduce a trigonometric parameterization $K = \cos \phi$ and $\Gamma = \sin \phi$ and focus on the range $0 \leq \phi/\pi \leq 3/4$.

Yang et al. [34, 40] have extensively studied the K Γ -chain limit and identified two relevant sublattice transformations: a six-sublattice transformation mapping the K Γ -chain to either the ferromagnetic Heisenberg (FMH) chain at $\phi/\pi = 3/4$ or the AFH chain at $\phi/\pi = -1/4$, and a three-sublattice transformation mapping $\Gamma \mapsto -\Gamma$ such that the phase diagram is symmetric about the pure Kitaev limits, $\phi \mapsto -\phi$. An emergent $SU(2)_1$ TLL phase

has been reported in a wide range, $0 < \phi/\pi < \pm 0.66$ [34], around the dual AFH points, $\phi/\pi = \pm 1/4$. While the $SU(2)$ symmetry is a property of the Hamiltonian at the dual points, the system retains the $SU(2)$ symmetry as an emergent property at any other ϕ within the TLL phase.

Methods. We make use of different numerical techniques and their respective cluster geometries [cf. Fig. 1 (c-f)] in a complementary way. Exact diagonalizations (ED) enables us to study the K Γ model on a C_3 -symmetric cluster with 24 sites. In the chain limit, the 24-site cluster decomposes into two chains with 12 sites each implying large finite-size gaps. With Density Matrix Renormalization Group (DMRG) [41] and the infinite matrix product state (iMPS) [42, 43] framework, on the other hand, we can treat chains of infinite length eliminating their finite-size gap. When comparing with ED, it is instructive to also consider a geometry with finite chains in DMRG. In the remainder of the text, we will refer to each geometry by the label given in Fig. 1 (c-f). On general grounds, we expect ED to be more reliable in obtaining the positions of the phase transitions near the C_3 limit, $d \approx 1$, due to maintaining the lattice symmetries. On the other hand, DMRG and iMPS are not limited by the finite-size gaps of K Γ chains at finite length and are expected to be more reliable for weakly coupled chains, $d \ll 1$. Furthermore, we compute dynamical spin-spin correlations employing a time evolution of matrix product states [44, 45] for the $\text{rho}_{(3,\infty)}$ geometry with three coupled chains.

Ground State. We start by focusing on the ground state properties at fixed $\phi/\pi = 1/4$, cf. Fig. 2. Near the chain-limit, $\text{ED}_{C_3,24}$ obtains a lower ground state energy in agreement with the finite-chain geometry $\text{rho}_{(\infty,12)}$ in DMRG. The finite-size gap is sizable for both geometries. Shortly before approaching the C_3 limit, $\text{rec}_{(4,\infty)}$ with

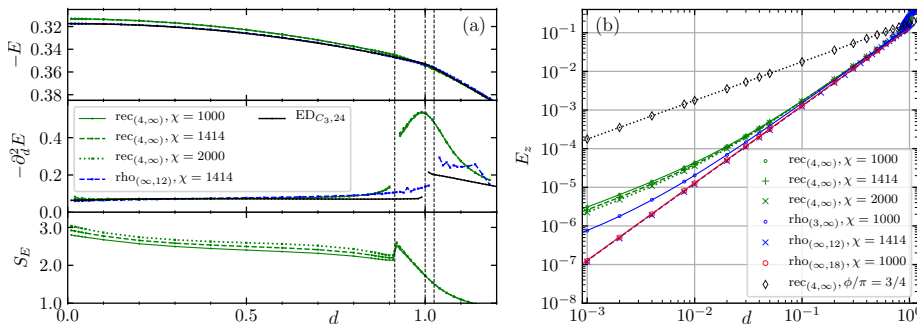


FIG. 2. (a) Representative cut through the phase diagram, Fig. 1, with constant $\phi/\pi = 1/4$ and varying inter-chain coupling d . ED (black) features a single transition at $d_c^{ED} = 1$ close to $d_c^{12} = 1.025$ of $\text{rec}_{(\infty,12)}$, whereas $\text{rec}_{(4,\infty)}$ exhibits two transitions at $d_{c,1}^\infty \approx 0.92$ and $d_{c,2}^\infty \approx 0.99$. For $d < d_{c,2}^\infty$, $\text{rec}_{(4,\infty)}$ (green) features a χ -dependence of the entanglement entropy of a bipartition, S_E , suggesting a gapless phase. (b) Contribution to the ground state energy from the z-bond, E_z , scaling as $E_z \propto d^2$, while E_z scales linearly, $E_z \propto d$, in the vertex phase near $\phi/\pi = 3/4$. Lines in (b) are fits with parameters listed in table (c).

infinite chains obtains a lower ground state energy until eventually the ground state energies for all geometries converge to a single line for $d \gtrsim 1.1$ and finite-size effects become negligible.

The second derivative $\partial_d^2 E$ features only a single phase transition at $d_c^{ED} = 1$ for $\text{ED}_{C_{3,24}}$ and at $d_c^{12} = 1.025$ for $\text{rho}_{(\infty,12)}$. The results on $\text{rec}_{(4,\infty)}$ exhibit two features: A kink originating from a first-order transition near $d_{c,1}^\infty = 0.92$ and a broad peak around $d_{c,2}^\infty \approx 0.99$. The entanglement entropy of a bipartition, S_E , is particularly enhanced for $d < d_{c,1}^\infty$, which connects to the chain limit. Here, S_E depends on the bond dimension, χ , in a way that is consistent with a gapless phase; $S_E(\chi)$ follows equidistant lines if χ is increased exponentially, $\chi = \{1000, 1414, 2000\} \approx 2^{n/2} \cdot 1000$ with $n = 0, 1, 2$. S_E drops off quickly upon increasing d beyond $d_{c,1}^\infty$ and S_E ceases to depend on χ , which implies a gapped phase. A spectral gap is expected for $d > 1$ due to its adiabatic connection to a product state of triplet states [46] with quadrupolar order [47]. In the case of $\text{rec}_{(4,\infty)}$, finite-size effects are most pronounced for $d \approx 1$, likely resulting in a finite-size gap already for $d < 1$ and the sequence of transitions observed here.

We turn now to small inter-chain coupling, $d \rightarrow 0$. Figure 2(b) shows the energy at the inter-chain bond, E_z , as a function of d . By fitting the function $f(d) = c_1 d^2 + c_2 d$, we observe that E_z does depend quadratically on d at $\phi/\pi = 1/4$ within the QSL phase. This behaviour is most evident for the finite-chain geometries $\text{rho}_{(\infty,L)}$ with $L = \{12, 18\}$, while the infinite-chain geometries, $\text{rho}_{(3,\infty)}$ and $\text{rec}_{(4,\infty)}$, have small corrections to the quadratic behaviour which further reduce as χ is increased. In contrast, a linear scaling is expected for the magnetically long-range ordered phase at $\phi/\pi = 3/4$, as confirmed in Fig. 2(b).

Finding a quadratic, rather than a linear, dependence on d suggests that the dominant correlations along the chains compete with the inter-chain coupling. While suc-

cessive application of the six- and the three-sublattice rotation maps the KT chains to AFH chains along the x and y bonds [34], the exchange on z bonds maps to a Heisenberg-like diagonal exchange with a peculiar, positionally dependent modulation of the signs for each diagonal component. This modulation is not compatible with the dominant Néel-like correlations along the chain [48]. Likewise, a perturbative treatment of coupled chains appears to be challenging due to the high symmetry of the KT chain [49].

Extent of the QSL phase. Based on the ground-state energy $E = E(d, \phi)$ for the Hamiltonian (1), its first derivative $\partial_d E$ ($\partial_\phi E$), and its second derivative $\partial_d^2 E$ ($\partial_\phi^2 E$) against d (ϕ), we map out the extent of the QSL phase originating from the TLL, cf. Fig. 1(a). The ferromagnetic KSL at $\phi = 0$ is very fragile against the Γ interaction, which is consistent with earlier results at $d = 1$ [7, 26, 50]. Results for $\text{ED}_{C_{3,24}}$ suggest a direct transition between KSL and QSL for $0 < d < 0.9$, while for $\text{rec}_{(4,\infty)}$ an intermediate phase exists with a dimerization along the x and y bonds for $\phi/\pi < 0.02$ at small $d \lesssim 0.2$, as well as an intermediate trivial paramagnet for $0.3 \lesssim d \lesssim 1$ and $\phi/\pi < 0.05$.

In the chain limit, $d = 0$, the TLL phase appears for 0 (0.02) $< \phi/\pi < 0.66$ in ED (DMRG). A long-range ordered phase with D_4 symmetry (D4FM) stabilizes at $0.69 \lesssim \phi/\pi < 0.88$ around the FMH dual point [34]. When $d > 0$ D4FM turns into a long-range ordered phase with non-coplanar 90° order. In contrast to Refs. [34, 40], we find an additional region with strong incommensurate correlations between TLL and D4FM, which survives small inter-chain coupling $d \lesssim 0.05$. For $0.05 \lesssim d < d_{c,\text{IM2}} \approx 0.8$ (0.6), $\text{ED}_{C_{3,24}}$ ($\text{rec}_{(4,\infty)}$) shows a direct first-order transition between QSL and the non-coplanar order. A second intermediate phase stabilizes for $d > d_{c,\text{IM2}}$, which is characterized by the absence of local magnetic moments, and a critical scaling consistent with a gapless spectrum [48].

Near the C_3 limit, $d \approx 1$, ED and DMRG results show qualitative differences. $\text{ED}_{C_3,24}$ features a single transition between the QSL and a trivial paramagnet (PM) at $d = 1$ in a wide range $0.2 \lesssim \phi/\pi \lesssim 0.6$. The PM phase is connected adiabatically to the triplet-dimer limit at $d \rightarrow \infty$ [46]. On the other hand, $\text{rec}_{(4,\infty)}$ features two transitions: a kink in $\partial_d^2 E$ at $d \approx 0.9$ to 0.95 , and a broad feature near $d \approx 1$. Both transitions merge into a single kink at $d \approx 0.95$ for $\phi/\pi \gtrsim 0.3$.

iMPS χ -Scaling. In the following, we utilize the procedure outlined in Refs. [51, 52] to extract the spectral gap by using the eigenvalues of an iMPS transfer matrix (TM) which contain full information about the equal-time correlations [53, 54]. For Hamiltonians with only local interactions, the equal-time correlations are related to the spectral gap [55], $\xi \sim 1/\Delta$. This statement has been extended by Zauner et al. [53] to include momentum, such that $\xi(\mathbf{k}) \sim 1/\Delta(\mathbf{k})$ in the vicinity of \mathbf{k} . Moreover, if the symmetry upon translation along the cylinder circumference is not broken, then for each $k_y = 2\pi/L_y$ a set of TM-eigenvalues λ_i exists with a longitudinal momentum $k_x = \arg \lambda_i$ corresponding to the momentum at a minimum of the spectrum. Here, we are sorting λ_i by their momenta $\mathbf{k} = (k_x, k_y)$, and only use λ_i for $k_x \approx 2\pi/3$ and $k_y = 0$, where we obtain the smallest $\epsilon_{\mathbf{k}} = \epsilon_{0,\mathbf{k}} = 1/\lambda_1$, corresponding to the dominant correlations.

We find $\epsilon_{\mathbf{k}}(\chi)$ to decrease as a function of the spacing between the inverse eigenvalues, $\delta_{\mathbf{k}}(\chi) = \sum_i c_i \epsilon_{i,\mathbf{k}}$, where $\sum_i c_i = 0$. The results are shown in Fig. 3(a). Solid lines represent fits to the function $f(\delta) = c_1 \delta^{c_2} + c_0$. In all cases, we observe an almost linear behaviour with $c_2 = 1.0(1)$ and $c_0 = 0.00(3)$ consistent with a gapless nature of the QSL. For comparison, we include similar data for a single K Γ chain whose ground state is a gapless $SU(2)_1$ TLL with a well defined scaling form. Moreover, we confirm that local magnetic moments vanish in the $\chi \rightarrow \infty$ limit, ruling out long-range magnetic order [48].

Dynamical properties. At $\phi/\pi = 1/4$, where the K Γ chain is equivalent to the AFH chain, the excitations are spin-1/2 spinons with the characteristic continuum in the dynamical spin structure factor (DSF) bounded by a double arc and linear dispersion at the gapless points [56–59]. As shown in Fig. 3(b), the K Γ chain features three copies of the AFH chain spectrum due to a tripling of the unit cell by the six-sublattice transformation. For coupled infinite chains—here, we use $\text{rho}_{(3,\infty)}$ at $d = 0.5$ —the DSF retains these features [60]. Within bounds set by the resolution, the DSF remains gapless with linear dispersion at $\mathbf{k} = \{\Gamma, \frac{2}{3}M, \frac{4}{3}M, \Gamma'\}$. The broad continuum is mostly unchanged apart from a shift of some spectral weight to low energies at Γ' . Upon tuning towards either $\Gamma \rightarrow 0$ or $K \rightarrow 0$, the lower edge of the spectrum flattens, while maintaining the same arc-like lower boundary with linear gapless modes. At $\phi/\pi = 0.1$, the upper edge of the continuum moves towards lower energies ($\omega_{\max} \approx 2$) approaching the upper cutoff known for the KSL [61, 62].

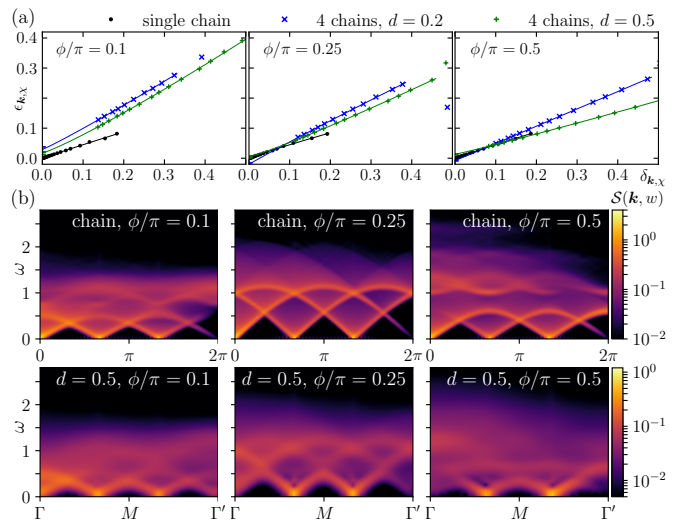


FIG. 3. (a) The spectral gap $\epsilon_{\mathbf{k}}(\chi)$ at $\mathbf{k} = (2\pi/3, 0)$ extracted from the transfer matrix of the iMPS vanishes linearly with $\delta_{\mathbf{k}}(\chi)$ as $\chi \rightarrow \infty$ similar to the K Γ -chain (black). We confirm these results at $\phi/\pi = \{0.1, 0.25, 0.5\}$ using $\text{rec}_{(4,\infty)}$ at $d = 0.2$ (blue) and 0.5 (green). (b) Dynamical spin-structure factor $\mathcal{S}(\mathbf{k}, \omega)$ for the K Γ -chain (top), and $\text{rho}_{(3,\infty)}$ at $d = 0.5$ (bottom). At $\phi/\pi = 1/4$ the K Γ -chain is equivalent to the AFH chain with its characteristic spinon continuum. The six-sublattice transformation results in three instances of the spinon spectrum shifted by $\delta k_x = \pm 2\pi/3$. Within the resolution limit ($\sigma_\omega = 0.080$), the linear gapless modes and the spinon continuum persists for finite inter chain coupling.

At $\phi/\pi = 0.5$, on the other hand, the upper edge moves to higher energies, and a second dispersive feature develops at $1 < \omega < 1.4$.

We interpret the similarities in the DSF between coupled chains and the K Γ -chain as a signature of the excitations being of the same spinon nature. Although changing ϕ changes the DSF notably, the qualitative behaviour—and, thus, the nature of the excitations—at low-energies remains similar.

Discussion. We have provided numerical evidence for the existence of an extended QSL phase born out of the emergent TLL phase in the one-dimensional limit. Competing spin exchanges due to the inter-chain coupling lead to frustration, suppress long-range magnetic order, and stabilize a QSL with spinon-like excitations. Remarkably, this phase extends up to the C_3 limit.

One may argue that additional exchanges, such as Heisenberg, Γ' , or further-neighbor exchanges, will act as a singular perturbation and stabilize long-range magnetic order [49]. However, we want to highlight the possible relation of the QSL reported here with the lattice-nematic paramagnet (NP) found in a K $\Gamma\Gamma'$ model in applied magnetic field along the [111] axis [24, 27]. There, upon adding a small negative Γ' , the NP phase gives way to zigzag magnetic order at low field, while NP reappears once the applied magnetic field suppresses the magnetic

order.

This has important implications on possible realisations in materials: (i) the QSL exists in a wide region of mostly ferromagnetic Kitaev and antiferro-like Γ exchange and in an applied external magnetic field. When the crystal symmetry remains (close to) C_3 , applying a magnetic field along the [111] axis (or c^* axis) and tuning the tilting angle appropriately can select the NP state that corresponds to this QSL [27]. (ii) the QSL may be stabilized in Kitaev materials with a from C_3 down to C_2 reduced space-group symmetry. Such a reduction can be intrinsic due to a reduced crystal symmetry. Alternatively, applying a uniaxial strain or an external magnetic field will alter the spin-exchange via magnetoelastic coupling [31, 32].

Acknowledgements. This work was supported by JSPS KAKENHI (Grants No. 21K03390 and 22K14008) from MEXT, Japan. We acknowledge the use of computational resources of the supercomputer Fugaku provided by the RIKEN AICS through the HPCI System Research Project (Project ID: hp210321), of the ISSP Supercomputer Center at the University of Tokyo, and of the Scientific Computing section of the Research Support Division at the Okinawa Institute of Science and Technology Graduate University (OIST). M.G. acknowledges support by the Theory of Quantum Matter Unit at OIST.

-
- [1] L. Balents, Spin liquids in frustrated magnets, *Nature* **464**, 199 (2010).
- [2] L. Savary and L. Balents, Quantum Spin Liquids: A Review, *Rep. Prog. Phys.* **80**, 016502 (2017).
- [3] J. Knolle and R. Moessner, A Field Guide to Spin Liquids, *Annual Review of Condensed Matter Physics* **10**, 451 (2019).
- [4] P. W. Anderson, The resonating valence bond state in La_2CuO_4 and superconductivity, *Science* **235**, 1196 (1987).
- [5] A. Kitaev, Anyons in an Exactly Solved Model and Beyond, *Ann. Phys. (NY)* **321**, 2 (2006).
- [6] G. Jackeli and G. Khaliullin, Mott Insulators in the Strong Spin-Orbit Coupling Limit: From Heisenberg to a Quantum Compass and Kitaev Models, *Phys. Rev. Lett.* **102**, 017205 (2009).
- [7] J. G. Rau, E. K.-H. Lee, and H.-Y. Kee, Generic Spin Model for the Honeycomb Iridates beyond the Kitaev Limit, *Phys. Rev. Lett.* **112**, 077204 (2014).
- [8] S. Trebst, Kitaev Materials, *ArXiv e-prints* (2017), arXiv:1701.07056 [cond-mat.str-el].
- [9] S. M. Winter, A. A. Tsirlin, M. Daghofer, J. van den Brink, Y. Singh, P. Gegenwart, and R. Valentí, Models and materials for generalized Kitaev magnetism, *Journal of Physics: Condensed Matter* **29**, 493002 (2017).
- [10] M. Hermanns, I. Kimchi, and J. Knolle, Physics of the Kitaev Model: Fractionalization, Dynamic Correlations, and Material Connections, *Annual Review of Condensed Matter Physics* **9**, 17 (2018).
- [11] Y. Motome, R. Sano, S. Jang, Y. Sugita, and Y. Kato, Materials design of Kitaev spin liquids beyond the Jackeli–Khaliullin mechanism, *J. Phys.: Condens. Matter* **32**, 404001 (2020).
- [12] K. W. Plumb, J. P. Clancy, L. J. Sandilands, V. V. Shankar, Y. F. Hu, K. S. Burch, H.-Y. Kee, and Y.-J. Kim, α - RuCl_3 : A spin-orbit assisted Mott insulator on a honeycomb lattice, *Phys. Rev. B* **90**, 041112(R) (2014).
- [13] S.-H. Baek, S.-H. Do, K.-Y. Choi, Y. S. Kwon, A. U. B. Wolter, S. Nishimoto, J. van den Brink, and B. Büchner, Evidence for a Field-Induced Quantum Spin Liquid in α - RuCl_3 , *Phys. Rev. Lett.* **119**, 037201 (2017).
- [14] A. Banerjee, P. Lampen-Kelley, J. Knolle, C. Balz, A. A. Aczel, B. Winn, Y. Liu, D. Pajerowski, J. Yan, C. A. Bridges, A. T. Savici, B. C. Chakoumakos, M. D. Lumsden, D. A. Tennant, R. Moessner, D. G. Mandrus, and S. E. Nagler, Excitations in the field-induced quantum spin liquid state of α - RuCl_3 , *npj Quantum Materials* **3**, 8 (2018).
- [15] Y. Kasahara, T. Ohnishi, Y. Mizukami, O. Tanaka, S. Ma, K. Sugii, N. Kurita, H. Tanaka, J. Nasu, Y. Motome, T. Shibauchi, and Y. Matsuda, Majorana Quantization and Half-Integer Thermal Quantum Hall Effect in a Kitaev Spin Liquid, *Nature* **559**, 227 (2018).
- [16] M. Yamashita, J. Gouchi, Y. Uwatoko, N. Kurita, and H. Tanaka, Sample dependence of half-integer quantized thermal Hall effect in the Kitaev spin-liquid candidate α - RuCl_3 , *Phys. Rev. B* **102**, 220404 (2020).
- [17] T. Yokoi, S. Ma, Y. Kasahara, S. Kasahara, T. Shibauchi, N. Kurita, H. Tanaka, J. Nasu, Y. Motome, C. Hickey, S. Trebst, and Y. Matsuda, Half-integer quantized anomalous thermal Hall effect in the Kitaev material candidate α - RuCl_3 , *Science* **373**, 568 (2021).
- [18] J. A. N. Bruin, R. R. Claus, Y. Matsumoto, N. Kurita, H. Tanaka, and H. Takagi, Robustness of the thermal Hall effect close to half-quantization in α - RuCl_3 , *Nature Physics* **18**, 401 (2022).
- [19] K. Ran, J. Wang, W. Wang, Z.-Y. Dong, X. Ren, S. Bao, S. Li, Z. Ma, Y. Gan, Y. Zhang, J. T. Park, G. Deng, S. Danilkin, S.-L. Yu, J.-X. Li, and J. Wen, Spin-Wave Excitations Evidencing the Kitaev Interaction in Single Crystalline α - RuCl_3 , *Phys. Rev. Lett.* **118**, 107203 (2017).
- [20] L. Janssen, E. C. Andrade, and M. Vojta, Magnetization processes of zigzag states on the honeycomb lattice: Identifying spin models for α - RuCl_3 and Na_2IrO_3 , *Phys. Rev. B* **96**, 064430 (2017).
- [21] W. Wang, Z.-Y. Dong, S.-L. Yu, and J.-X. Li, Theoretical investigation of magnetic dynamics in α - RuCl_3 , *Phys. Rev. B* **96**, 115103 (2017).
- [22] S. M. Winter, K. Riedl, P. A. Maksimov, A. L. Chernyshev, A. Honecker, and R. Valenti, Breakdown of magnons in a strongly spin-orbital coupled magnet, *Nature Communications* **8**, 1152 (2017).
- [23] J. Wang, B. Normand, and Z.-X. Liu, One Proximate Kitaev Spin Liquid in the K - J - Γ Model on the Honeycomb Lattice, *Phys. Rev. Lett.* **123**, 197201 (2019).
- [24] H.-Y. Lee, R. Kaneko, L. E. Chern, T. Okubo, Y. Yamaji, N. Kawashima, and Y. B. Kim, Magnetic-Field Induced Quantum Phases in Tensor Network Study of Kitaev Magnets, arXiv:1908.07671 [cond-mat] (2019).
- [25] F. L. Buessen and Y. B. Kim, Functional renormalization group study of the Kitaev- Γ model on the honeycomb lattice and emergent incommensurate magnetic correlations, *Phys. Rev. B* **103**, 184407 (2021).

- [26] M. Gohlke, G. Wachtel, Y. Yamaji, F. Pollmann, and Y. B. Kim, Quantum spin liquid signatures in Kitaev-like frustrated magnets, *Phys. Rev. B* **97**, 075126 (2018).
- [27] M. Gohlke, L. E. Chern, H.-Y. Kee, and Y. B. Kim, Emergence of nematic paramagnet via quantum order-by-disorder and pseudo-Goldstone modes in Kitaev magnets, *Phys. Rev. Research* **2**, 043023 (2020).
- [28] R. D. Johnson, S. C. Williams, A. A. Haghighirad, J. Singleton, V. Zapf, P. Manuel, I. I. Mazin, Y. Li, H. O. Jeschke, R. Valentí, and R. Coldea, Monoclinic crystal structure of α -RuCl₃ and the zigzag antiferromagnetic ground state, *Phys. Rev. B* **92**, 235119 (2015).
- [29] H. B. Cao, A. Banerjee, J.-Q. Yan, C. A. Bridges, M. D. Lumsden, D. G. Mandrus, D. A. Tennant, B. C. Chakoumakos, and S. E. Nagler, Low-temperature crystal and magnetic structure of α -RuCl₃, *Phys. Rev. B* **93**, 134423 (2016).
- [30] L. Janssen, S. Koch, and M. Vojta, Magnon dispersion and dynamic spin response in three-dimensional spin models for α -RuCl₃, *Phys. Rev. B* **101**, 174444 (2020).
- [31] V. Kocsis, D. A. S. Kaib, K. Riedl, S. Gass, P. Lampen-Kelley, D. G. Mandrus, S. E. Nagler, N. Pérez, K. Nielsch, B. Büchner, A. U. B. Wolter, and R. Valentí, Magnetoelastic coupling anisotropy in the Kitaev material α -RuCl₃, *Phys. Rev. B* **105**, 094410 (2022).
- [32] D. A. S. Kaib, S. Biswas, K. Riedl, S. M. Winter, and R. Valentí, Magnetoelastic coupling and effects of uniaxial strain in α -RuCl₃ from first principles, *Phys. Rev. B* **103**, L140402 (2021).
- [33] J. Wang and Z.-X. Liu, Symmetry-protected gapless spin liquids on the strained honeycomb lattice, *Phys. Rev. B* **102**, 094416 (2020).
- [34] W. Yang, A. Nocera, T. Tummuru, H.-Y. Kee, and I. Affleck, Phase Diagram of the Spin-1/2 Kitaev-Gamma Chain and Emergent SU(2) Symmetry, *Phys. Rev. Lett.* **124**, 147205 (2020).
- [35] T. Giamarchi, *Quantum Physics in One Dimension*, International Series of Monographs on Physics (Clarendon Press, 2003).
- [36] H. J. Schulz, Dynamics of Coupled Quantum Spin Chains, *Phys. Rev. Lett.* **77**, 2790 (1996).
- [37] V. J. Emery, E. Fradkin, S. A. Kivelson, and T. C. Lubensky, Quantum Theory of the Smectic Metal State in Stripe Phases, *Phys. Rev. Lett.* **85**, 2160 (2000).
- [38] A. Vishwanath and D. Carpentier, Two-Dimensional Anisotropic Non-Fermi-Liquid Phase of Coupled Luttinger Liquids, *Phys. Rev. Lett.* **86**, 676 (2001).
- [39] R. Mukhopadhyay, C. L. Kane, and T. C. Lubensky, Sliding Luttinger liquid phases, *Phys. Rev. B* **64**, 045120 (2001).
- [40] W. Yang, A. Nocera, and I. Affleck, Comprehensive study of the phase diagram of the spin- $\frac{1}{2}$ Kitaev-Heisenberg-Gamma chain, *Phys. Rev. Research* **2**, 033268 (2020).
- [41] S. R. White, Density Matrix Formulation for Quantum Renormalization Groups, *Phys. Rev. Lett.* **69**, 2863 (1992).
- [42] I. P. McCulloch, Infinite Size Density Matrix Renormalization Group, Revisited (2008).
- [43] H. N. Phien, G. Vidal, and I. P. McCulloch, Infinite Boundary Conditions for Matrix Product State Calculations, *Phys. Rev. B* **86**, 245107 (2012).
- [44] M. P. Zaletel, R. S. K. Mong, C. Karrasch, J. E. Moore, and F. Pollmann, Time-Evolving a Matrix Product State with Long-Ranged Interactions, *Phys. Rev. B* **91**, 165112 (2015).
- [45] M. Gohlke, R. Verresen, R. Moessner, and F. Pollmann, Dynamics of the Kitaev-Heisenberg Model, *Phys. Rev. Lett.* **119**, 157203 (2017).
- [46] T. Yamada, T. Suzuki, and S.-i. Suga, Ground-state properties of the $K - \Gamma$ model on a honeycomb lattice, *Phys. Rev. B* **102**, 024415 (2020).
- [47] A. Andreev and I. Grishchuk, Spin nematics, *Sov. Phys. JETP* **60**, 267 (1984).
- [48] M. Gohlke, J. C. Pelayo, and T. Suzuki, (in preparation).
- [49] W. Yang, A. Nocera, C. Xu, H.-Y. Kee, and I. Affleck, Counter-rotating spiral, zigzag, and 120° orders from coupled-chain analysis of Kitaev-Gamma-Heisenberg model, and relations to honeycomb iridates, arXiv:2207.02188 (2022).
- [50] S.-S. Zhang, G. B. Halász, W. Zhu, and C. D. Batista, Variational study of the Kitaev-Heisenberg-Gamma model, *Phys. Rev. B* **104**, 014411 (2021).
- [51] M. M. Rams, P. Czarnik, and L. Cincio, Precise Extrapolation of the Correlation Function Asymptotics in Uniform Tensor Network States with Application to the Bose-Hubbard and XXZ Models, *Phys. Rev. X* **8**, 041033 (2018).
- [52] B. Vanhecke, J. Haegeman, K. Van Acoleyen, L. Vanderstraeten, and F. Verstraete, Scaling Hypothesis for Matrix Product States, *Phys. Rev. Lett.* **123**, 250604 (2019).
- [53] V. Zauner, D. Draxler, L. Vanderstraeten, M. Degroote, J. Haegeman, M. M. Rams, V. Stojevic, N. Schuch, and F. Verstraete, Transfer matrices and excitations with matrix product states, *New J. Phys.* **17**, 053002 (2015).
- [54] Y.-C. He, M. P. Zaletel, M. Oshikawa, and F. Pollmann, Signatures of Dirac Cones in a DMRG Study of the Kagome Heisenberg Model, *Physical Review X* **7**, 031020 (2017).
- [55] M. B. Hastings, Locality in Quantum and Markov Dynamics on Lattices and Networks, *Phys. Rev. Lett.* **93**, 140402 (2004).
- [56] H. Bethe, Zur Theorie der Metalle, *Z. Phys.* **71**, 205 (1931).
- [57] T. Yamada, Fermi-Liquid Theory of Linear Antiferromagnetic Chains, *Progress of Theoretical Physics* **41**, 880 (1969).
- [58] G. Müller, H. Thomas, H. Beck, and J. C. Bonner, Quantum spin dynamics of the antiferromagnetic linear chain in zero and nonzero magnetic field, *Phys. Rev. B* **24**, 1429 (1981).
- [59] M. Karbach, G. Müller, A. H. Bougourzi, A. Fledderjohann, and K.-H. Mütter, Two-spinon dynamic structure factor of the one-dimensional $S = \frac{1}{2}$ Heisenberg antiferromagnet, *Phys. Rev. B* **55**, 12510 (1997).
- [60] Apart from an intrinsic broadening set by the longest times reached within the numerical simulations.
- [61] J. Knolle, D. Kovrizhin, J. Chalker, and R. Moessner, Dynamics of a Two-Dimensional Quantum Spin Liquid: Signatures of Emergent Majorana Fermions and Fluxes, *Phys. Rev. Lett.* **112**, 207203 (2014).
- [62] J. Knolle, D. L. Kovrizhin, J. T. Chalker, and R. Moessner, Dynamics of fractionalization in quantum spin liquids, *Phys. Rev. B* **92**, 115127 (2015).